

BayesBeat: A Bayesian Deep Learning Approach for Atrial Fibrillation Detection from Noisy Photoplethysmography Data

Sarkar Snigdha Sarathi Das, Subangkar Karmaker Shanto, Masum Rahman, Md Saiful Islam, Atif Rahman, Mohammad Mehedy Masud, and Mohammed Eunos Ali

Abstract—The increasing popularity of smartwatches as affordable and longitudinal monitoring devices enables us to capture photoplethysmography (PPG) sensor data for detecting Atrial Fibrillation (AF) in real-time. A significant challenge in AF detection from PPG signals comes from the inherent noise in the smartwatch PPG signals. In this paper, we propose a novel deep learning based approach, BayesBeat that leverages the power of Bayesian deep learning to accurately infer AF risks from noisy PPG signals, and at the same time provide the uncertainty estimate of the prediction. Bayesbeat is efficient, robust, flexible, and highly scalable which makes it particularly suitable for deployment in commercially available wearable devices. Extensive experiments on a recently published large dataset involving over 170 individuals reveal that our proposed method BayesBeat substantially outperforms the existing state-of-the-art methods.

Index Terms—Atrial fibrillation, Bayesian deep learning, convolutional neural network, photoplethysmography, PPG, uncertainty estimation

I. INTRODUCTION

ATRIAL fibrillation (AF) is the most prevalent form of arrhythmia, a type of heart disease, characterized by inconsistent beating pattern and abnormal heart activity. Early diagnosis of AF can significantly reduce the risk of death from a cardiac attack. As most of the AF events are asymptomatic at the initial stage, periodic clinical ECG assessment has a very low likelihood of detecting paroxysmal AF [1]. The increasing popularity of smartwatches or fitness trackers equipped with photoplethysmography (PPG) sensors opens a new opportunity for developing non-invasive continuous monitoring of AF from PPG signals.

This work was supported by Department of Information and Communication Technology (ICT), Bangladesh.

Sarkar Snigdha Sarathi Das, Subangkar Karmaker Shanto, and Masum Rahman are with the Department of Computer Science and Engineering, Bangladesh University of Engineering and Technology, Dhaka, Bangladesh. (e-mail: sarathismg, subangkar.karmaker, masum-rahman99@gmail.com).

Md Saiful Islam, Atif Rahman, and Mohammed Eunos Ali are with the Department of Computer Science and Engineering, Bangladesh University of Engineering and Technology, Dhaka, Bangladesh. (e-mail: saifulislam, atif, eunos@cse.buet.ac.bd).

Mohammad Mehedy Masud is with College of Information Technology, United Arab Emirates University, Al Ain, United Arab Emirates. (e-mail: m.masud@uaeu.ac.ae).

PPG sensors essentially use reflection intensity of emitted light with the body part to monitor volumetric blood flow alterations, which are ultimately converted to heart rate and heart beating patterns. Hence, proper contact with the body is fundamental to capturing noise-free signals. However, several recent studies show that motion artifacts during activities can significantly deteriorate the accuracy of heart rate calculation [2], [3]. Furthermore, skin tone [4], [5] and fastening belt pressure [6] have also been attributed to the source of noise in PPG signals.

Hence, both noise artifacts and the existence of AF can cause irregular pulse-to-pulse interval in PPG signals, which pose a major challenge in detecting AF from the captured signals.

A large body of research works in this domain rely on hand-crafted feature extraction from PPG signal to differentiate between AF and non-AF signals [7]–[10]. These approaches do not yield satisfactory prediction performance as high noise negatively affects the feature extraction phases. Inspired by the success of deep learning based techniques in ECG classification, a few recent approaches apply deep convolutional neural network (CNN) for prediction of risks from smartwatch PPG data [11]–[13].

Aliamiri and Shen [12] collected PPG signals in a controlled environment and filtered out the poor quality signals to increase detection accuracy. As this solution was not suitable for deployment in ambulatory setting, the authors later proposed to use ResNeXt [14] architecture without any explicit filtering step [13]. However, since significant portions of PPG signals are noisy the proposed model fails to accurately infer AF labels for those segments.

To address the issue of noise, Elgendi *et al.* proposed a signal quality index that categorizes PPG signals into three classes: excellent, acceptable (good), and unfit (poor) for diagnosis [16]. In a recent work [15], Torres *et al.* proposed a multi-task approach, where they first estimate the signal quality, and then in the next phase, detect AF with signals that are of excellent qualities. This state-of-the-art work has several limitations. They learn signal quality estimation in a supervised manner that requires huge human involvement for quality label annotation. To reduce the human effort, they manually annotate a part of the dataset using [16] and then label the rest of the dataset using a separate model trained on

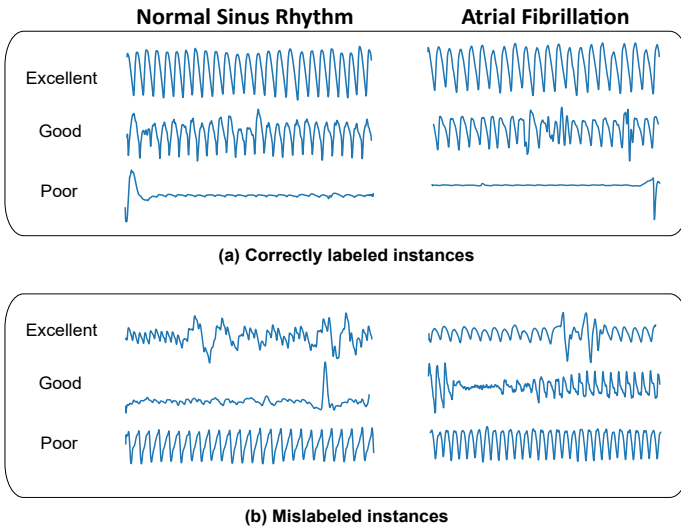


Fig. 1: Samples of PPG signals from the Stanford Wrist Photoplethysmography dataset [15]. Left column signals refer to normal sinus rhythm from healthy patients whereas right column signals are from subjects with Atrial Fibrillation. Torres *et al.* leveraged a semi-supervised scheme to automatically label the signal quality as Excellent, Good, or Poor. Although many signals are labeled correctly as in (a), this scheme makes frequent mistakes and labels many signals incorrectly, showed in (b).

the human-labeled dataset. However, this automated labeling approach may generate imprecise quality labels. Figures 1 (a) and (b) shows some of the signals that are *correctly labeled* and *wrongly labeled*, respectively, as excellent, good, and poor quality.

These inaccurate ground truth quality labels may propagate errors to the downstream model resulting in performance degradation. The proposed model also does not generalize well across the whole dataset, i.e., the results are excellent in test set, however, validation and training set results are not satisfactory.

To overcome the above limitations of handling uncertain PPG sensor data, in this paper, we propose a novel Bayesian deep learning approach, *BayesBeat* to provide a probabilistic guarantee of AF detection. The key intuition of our approach is to exploit the Bayesian deep learning based approach to capture the inherent uncertainty in the noisy PPG signals and take this uncertainty into account while detecting AF from PPG signals, rather than training separate models to assess the signal quality. The advantage of *BayesBeat* is multi-fold: (i) **robust**: can handle noisy PPG data and also avoid over-fitting for a small dataset, (ii) **efficient and scalable**: requires much fewer parameters, yet achieves state-of-art performance guarantee, which makes it suitable for low-end handheld devices, and (iii) **uncertainty guarantee**: gives aleatoric uncertainty (i.e. stochasticity of data resulting from input noise), which obviates the requirement of any supervision for signal quality estimation as the model itself learns to distinguish between AF related and motion-induced irregularities in PPG signals.

We have conducted an extensive set of experiments with

our model and compared it against the state-of-the-art AF detection algorithms with the largest publicly available Stanford wrist photoplethysmography dataset [15]. Our proposed model BayesBeat significantly outperforms state-of-the-art AF detection methods achieving 7.1-9.2% higher F1-score than [13] and 10-20% higher F1-score than [15].

In summary, we have made the following contributions:

- We propose a novel deep learning based approach, namely BayesBeat, to automatically detect AF from PPG signals.
- BayesBeat provides an uncertainty guarantee of the prediction, which can be handy in a real-world setting with noisy PPG data.
- Our experimental results show that BayesBeat requires significantly less number of parameters, and outperforms state-of-the-art methods, which makes it suitable for low-end wearable devices.

II. RELATED WORK

Existing works on AF detection from PPG data can be divided into three categories: traditional statistical analysis, classical machine learning (ML) based methods, and deep learning (DL) based methods.

Traditional Statistical Analysis Approaches: Most of the statistical approaches involved extracting different features from rhythm data, e.g. R to R interval, Shannon entropy, RMSSD, Poincare plot, etc. Each of these features was analyzed extensively to determine thresholds for Atrial Fibrillation detection [17], [18]. To handle noise artifacts in extracted signals, some later works also added movement detection to fix the thresholds [19], [20]. However, such simple measures did not achieve clinically useful performance in AF detection. **Classical Machine Learning based Approaches:** To improve performance over statistical approaches, several machine learning algorithms have been applied to comprehensive features extracted from PPG data. SVM [7], [8], logistic models [21]–[23], KNN [9], decision trees [10] have replaced traditional threshold-based detection allowing to capture complex relationship between different parameters. However, the success of these methods relied heavily on elaborate feature engineering by domain experts, which is quite challenging for inherently noisy PPG signals due to motion artifacts.

Deep Learning (DL) based Approaches: Unlike other machine learning methods, deep learning algorithms can learn complex feature representations eliminating the requirement of hand-picked features. Consequently, state-of-the-art AF detection algorithms leverage deep learning for accurate prediction. Aliamiri and Shen [12] proposed a convolutional recurrent hybrid model for AF detection. They also used a separate quality assessment network for estimating signal quality. However, since they only worked with controlled environment data, it was not suitable for usage in an ambulatory noisy setting. To alleviate this problem, in a later work [13], they used 1D ResNeXt architecture [14], a model with over 7.5 million parameters which they found to be robust against noise artifacts. Nevertheless, a model that considers all signal segments equally is not practical in the real world setting, since a significant portion of signals gets heavily distorted by noise artifacts

from micro-movement, uneven skin contact, etc. Furthermore, a computation heavy model like ResNeXt is not suitable to be deployed in consumer devices with limited power. Poh. *et al.* [24] used convolutional neural network for AF prediction. However, their study was limited to fingertip PPG records in clinical setting, which are less susceptible to input noise. To assess the problems related to noise, recently Torres *et al.* [15] collected a large dataset involving both AF and non-AF individuals. Besides, for supervised training of signal quality, they labeled each signal segment with corresponding quality index [16]. This labeling process is partially done manually which is later utilized by a separate model for labeling the rest of the dataset. However, the automated labeling can be erroneous, and labeling errors can propagate to the final AF detection model leading to suboptimal performance.

III. PROBLEM FORMULATION

Let $X = \{X_k\}, k = 1, 2, \dots, N$ be the set of N PPG signal segments obtained from wearable PPG sensors. Each segment X_k is of length l , i.e., $X_k \in \mathbb{R}^l$. Our goal is to predict AF label $Y_k \in \{0, 1\}$, which represents negative (Normal Sinus Rhythm) or positive (Atrial Fibrillation), for each given $X_k \in X$. We refer to this as the Atrial Fibrillation (AF) detection problem.

A major challenge in AF detection from wearable PPG signals is the inherent noise due to the physical limitation of the current wearable technology and motion artifacts of the carrier. Figure 1 shows example signals from the Stanford wearable Photoplethysmography dataset [15], where we can see Excellent, Good, and Poor signals of both AF and non-AF categories. Existing methods [15] fail to capture these noises and sometimes mis-interpret these noises (Figure 1(b)), which may lead to poor performance in AF detection from noisy signals.

To overcome the above challenges in dealing with the varying degree of noise in input signals, we propose a Bayesian convolutional neural network architecture, *BayesBeat*. The key intuition of *BayesBeat* is to exploit the Bayesian deep learning based approach to capture the inherent uncertainty in the noisy PPG signals. Predictions on noisy signals are likely to yield high uncertainty scores. Hence the uncertainty score works as a proxy for signal quality, eliminating the need for a separate signal quality estimation model.

IV. OUR APPROACH: BAYESBEAT

In this section, we first give an overview of the Bayesian deep learning approach and then present the detailed formulation of our proposed Bayesian networks followed by the probabilistic inference. After that, we describe our *BayesBeat* architecture. Finally, we present our *BayesBeat* training algorithm.

A. Bayesian Deep Learning

Bayesian deep learning has recently shown its promise to capture uncertainty in real-world data by learning posterior distributions of the weights from training data sets. Formally,

given a training dataset \mathcal{D} , we first learn the posterior distribution of the weights $P(\mathbf{w}|\mathcal{D})$. Then, by using this posterior, the distribution of predicted label \mathbf{y}' given unseen test data \mathbf{x}' , is computed as $P(\mathbf{y}'|\mathbf{x}') = \mathbb{E}_{P(\mathbf{w}|\mathcal{D})}[P(\mathbf{y}'|\mathbf{x}', \mathbf{w})]$ [25].

However, computing the exact posterior requires the calculation of the probability of evidence $P(\mathcal{D})$, which is computationally intractable due to the high dimensionality of model parameters and real-world data. Hence, several techniques have been proposed for approximating posterior distribution [25]–[27]. Blundell *et al.* [25] proposed a backpropagation compatible algorithm *Bayes by backprop* for approximating the posteriors. Later Kingma *et al.* [26] employed a local reparameterization trick to achieve greater efficiency and lower variance gradient estimates. We adapt the above two techniques [25], [26] to model our posterior distribution and detect AF from PPG signals. Note that, Bayesian deep learning can also be achieved by using simple Monte Carlo dropout (Gal *et al.* [27]). However, recent studies suggest that this approach lacks expressiveness and does not fully capture the uncertainty in model predictions [28].

B. Modeling Bayesian Networks for BayesBeat

Unlike traditional deep learning layers that learn weights as points, all the parameter weights of our network are posterior probability distributions. As a result, the outputs of the network are probabilities from which we can calculate the uncertainty of a decision taken by the network. Figure 2(a) shows a high-level representation of how an input is transformed into output distributions by using a 1D Bayesian convolutional layer.

As the exact computation of posterior is intractable, our target is to approximate the true posterior $P(\mathbf{w}|\mathcal{D})$. For this, we first learn parameters θ for computing distribution of weights $q(\mathbf{w}|\theta)$ from which we can approximate $P(\mathbf{w}|\mathcal{D})$. To do this, we minimize the Kullback-Leibler (KL) divergence between $q(\mathbf{w}|\theta)$ and $P(\mathbf{w}|\mathcal{D})$, i.e., the goal is to minimize the cost function $\mathcal{F}(\mathcal{D}, \theta) = KL[q(\mathbf{w}|\theta) || P(\mathbf{w}|\mathcal{D})]$. After performing algebraic simplifications [25], the above minimization target can be expressed as follows:

$$\mathcal{F}(\mathcal{D}, \theta) = KL[q(\mathbf{w}|\theta) || P(\mathbf{w})] - \mathbb{E}_{q(\mathbf{w}|\theta)}[\log P(\mathcal{D}|\mathbf{w})] \quad (1)$$

The second term in this cost function is the negative log likelihood loss which depends on the dataset \mathcal{D} . On the other hand the first part depends on the selected prior $P(\mathbf{w})$ for the parameters. Following the strategies of previous works in Bayesian deep learning, we choose a simple prior $\mathcal{N}(0, I)$.

Since exact calculation of KL is also intractable, a closed form is formed from Equation 1 which approximates the KL by drawing n Monte Carlo samples:

$$\mathcal{F}(\mathcal{D}, \theta) \approx \sum_{k=1}^n \log q(\mathbf{w}^{(k)}|\theta) + \log P(\mathbf{w}^{(k)}) - \log P(\mathcal{D}|\mathbf{w}^{(k)}) \quad (2)$$

Here, $\mathbf{w}^{(k)}$ is the k^{th} Monte Carlo sample drawn from the posterior estimate $q(\mathbf{w}|\theta)$. Note that, cases where closed forms of KL can be computed, Equation 2 still performs equally well [25].

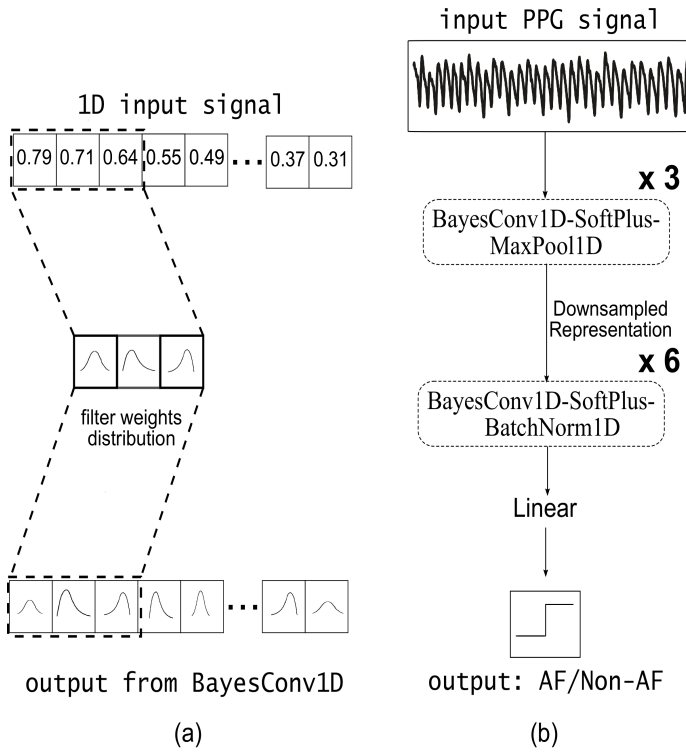


Fig. 2: (a) Illustration of a 1D Bayesian convolutional layer (BayesConv1D) of filter size 3. Here each weight in the convolution filter corresponds to a posterior distribution instead of a specific value. (b) Overview of our proposed *BayesBeat* architecture.

C. Inference

In the inference step, we calculate both the output probability and aleatoric uncertainty of the output decision (resulting from input noise). The output probability p' and the aleatoric uncertainty \ddot{u}_{al} can be estimated as follows (Kwon *et al.* [29]):

$$p' = \frac{1}{n} \sum_{k=1}^n \hat{p}_k \quad (3)$$

$$\ddot{u}_{al} = \frac{1}{n} \sum_{k=1}^n [\text{diag}(\hat{p}_k) - \hat{p}_k \hat{p}_k^T] \quad (4)$$

Here, $\hat{p}_k = \text{softmax}[f_{w_k}(x)]$ where w_k is the k th Monte Carlo sample weight drawn from the posteriors and x is the input signal.

D. BayesBeat Model Architecture

Figure 2(b) demonstrates the network architecture of *BayesBeat*. The network is composed of a total of nine Bayesian convolutional layers followed by fully connected layers. The first three of them contain maxpool operation to downsample the input signal removing redundant information and summarizing the key features. Other stages do not contain any pooling operation since downsampling the input too much may result in losing key features. At each stage, we employ *softplus* as our preferred activation function as it outperforms rectified linear unit (ReLU) in our case.

In Bayesian deep learning models, batch normalization and dropout can perturb the actual likelihood function, which may affect overall performance. We face similar outcomes with dropout as [30], i.e. incorporating dropout decreases model performance. However, batch normalization induces performance improvement. Consequently, batch normalization is employed for the final six stages of convolution while no dropout is employed at any stage of the network.

Algorithm 1: Training *BayesBeat* with *BBB*

Input: parameters, $\theta = (\mu, \rho)$, minibatches, $\mathcal{D} = \{\mathcal{D}_1, \mathcal{D}_2, \dots, \mathcal{D}_M\}$ number of draws, n
Output: Updated model parameters, θ_{out}

```

1 for  $i = 1 \rightarrow M$  do
2    $cost = 0$ 
3    $\lambda_i = \text{get\_Lambda}(i, M)$ 
4   for  $k = 1 \rightarrow n$  do
5     Sample  $\epsilon \sim \mathcal{N}(0, I)$ 
6      $w = \mu + \log[1 + \exp(\rho)] \circ \epsilon$ 
7      $term_{prior} = \log q(\mathbf{w}^{(k)} | \theta) + \log P(\mathbf{w}^{(k)})$  (Eq.
8       2)
9      $term_{likelihood} = -\log P(\mathcal{D} | \mathbf{w}^{(k)})$ 
10     $cost = cost + \lambda_i term_{prior} + term_{likelihood}$ 
11  find the gradients by backpropagating  $cost$  with
12  respect to  $\theta$ 
13  update parameters  $\theta = (\mu, \rho)$  with the computed
14  gradients
15  $\theta_{out} = \theta$ 

```

E. Training

The cost function in Equation 1 needs to be optimized by *minibatch gradient descent*. Since optimization has to be done on different minibatches of same size, the prior dependent part of Equation 1 requires to be weighted. Consequently, the cost function for minibatch i becomes:

$$\mathcal{F}_i(\mathcal{D}_i, \theta) = \lambda_i KL[q(\mathbf{w} | \theta) || P(\mathbf{w})] - \mathbb{E}_{q(\mathbf{w} | \theta)}[\log P(\mathcal{D}_i | \mathbf{w})] \quad (5)$$

The choice of $\lambda_i \in [0, 1]$ is a crucial factor for the performance of Bayesian deep learning models, which is an ongoing topic of research [30]. In our case $\lambda_i = 0$ induces overfitting and $\lambda_i = 1$ induces underfitting of the training dataset. Intuitively, these are expected as the KL term works like a regularization factor for the cost function. We also investigate different λ values proposed in [25], [31] and achieve the best performance from the one by Blundell *et al.* [25]. Consequently, we select $\lambda_i = \frac{2^{M-i}}{2^M - 1}$ scaled by a factor of 10^{-5} , where M is the total number of minibatches. We use the additional scaling term as smaller weights tend to perform better for several learning tasks [30].

We adapt the training pipeline of *BayesByBackprop(BBB)* [25] for training our model following the PyTorch implementation in [32]. The details of the training are presented in Algorithm 1. While Algorithm 1 performs reasonably well for the training, using local reparameterization

trick [26] on top of that makes training faster. Here, instead of sampling the weights, the activations are sampled, resulting in variance reduction of gradients. We chose $batch_size = 512$, and trained our network for 50 epochs with a learning rate of $1 \times e^{-3}$. For optimizer, we chose *Adam* [33]. During the training, the best model was selected based on the validation set performance. The whole model was trained using an i7-7700 workstation with 16 GB of RAM, and a GTX 1070 GPU for 1.5 days.

V. EXPERIMENTS

To test the efficacy of our proposed model *BayesBeat*, we extensively evaluate the performance of our approach and compare it with two state-of-the-art deep learning based approaches (Shen *et al.*, 2019 [13] and Torres *et al.*, 2020 [15]) for AF detection.

A. Dataset

To evaluate different models, we have used the largest publicly available dataset, which we refer to as the *Stanford Wearable Photoplethysmography Dataset*¹. This dataset is recently made public by Torres *et al.* with their work *DeepBeat* [15]. The dataset contains more than 500K signal segments from a total of 173 individuals (107 AF subjects and 66 non-AF subjects). Each of the data segments is 25s long sampled at 128 Hz and later downsampled to 32 Hz. These datasets contain sufficiently noisy signal segments that conform to the real-world settings in the ambulatory environment.

The dataset is also supplemented with three types of signal labels, i.e., Poor, Good, and Excellent. However, only a portion of them are labeled by human; the rest of them are generated from a model trained on the human-labeled portion. While this process makes it easy to label such a huge dataset, it also generates some imprecise labels in the dataset which can make downstream models vulnerable to error propagation. Figure 1 (b) shows such instances where the accompanying quality labels do not represent the true quality of the signal. Considering these pitfalls, instead of using the given labels, we use the uncertainty estimation from our *BayesBeat* model to account for the prediction.

Distribution and Pre-processing: We address some distribution issues present in the original train, validation, test split of the dataset. In the originally published dataset, the test set is extremely small and there are overlapping signal segments that introduce the repetition of the same segments in different test samples. Furthermore, the ratio of AF and non-AF subjects are also very different from that of the train and validation sets. Due to these issues, the test set can misrepresent the performance of a model. Because of these distribution issues, while the proposed model in [15] reported exceptional performance in test set (sensitivity: 0.98, specificity: 0.99, F1-score: 0.96), the performance is poor in the validation set (sensitivity: 0.59, specificity: 0.995, F1 score: 0.69) and train set (sensitivity: 0.59, specificity: 0.998, F1 score: 0.74).

To address these problems, we redistribute the whole dataset and split 70% of it as train, 15% as validation, and 15% as test sets. Furthermore, we removed all overlapping signal segments from the validation and test set to ascertain that the same windows are not counted multiple times during evaluation. No subjects were overlapping across train, validation, and test sets. In our distribution, the ratio of AF and non-AF segments in test set (0.39) is also very close to the actual dataset (0.38) which ensures that we get the actual representation of the performance.

For preprocessing, all the signals are first bandpass-filtered, and then the signal values are standardized to [0,1].

B. Evaluation Metrics and Baselines

To evaluate different models, we have used a wide range of metrics that include Recall (Sensitivity), Specificity (True Negative Rate, TNR), Precision (Positive Predictive Value, PPV), and F1-Score. These metrics can be formally expressed as follows.

$$\begin{aligned} \text{Recall} &= \frac{TP}{TP + FN} \\ \text{Specificity} &= \frac{TN}{TN + FP} \\ \text{Precision} &= \frac{TP}{TP + FP} \\ \text{F1} &= \frac{2 * (\text{Precision} * \text{Recall})}{\text{Precision} + \text{Recall}} \end{aligned}$$

Here, TP (True Positive) is the number of positive signals correctly classified by the model, TN (True Negative) is the number of negative signals correctly classified by the model, FP (False Positive) is the number of signals falsely classified as positive, and FN (False Negative) is the number of signals falsely classified as negative.

We also use AUC, area under ROC curve and *Matthews Correlation Coefficient (MCC)* as our evaluation metrics. Though AUC is commonly used in the prior works, it can give misleading performance representation for class imbalance dataset; whereas MCC is particularly effective in assessing the performance of a binary classifier in case of imbalanced data [34].

$$MCC = \frac{TP * TN - FP * FN}{\sqrt{(TP + FP)(TP + FN)(TN + FP)(TN + FN)}}$$

We compare our results against the most recent state-of-the-art works by Shen *et al.* [13] and Torres *et al.* [15]. For [13], we implemented the 1D ResNeXt architecture having over 7.5 million parameters with the same network and hyperparameter settings as stated in the paper. We found that this network fits the training data quite easily irrespective of signal quality, which eventually leads to overfitting. On the other hand, Torres *et al.* provided the architecture of their model “*DeepBeat*” which we first pre-train as in [15] and then train on the redistributed dataset. This baseline has a separate signal quality estimation part, with which the excellent quality signals can

¹<https://www.synapse.org/#!Synapse:syn21985690/files/>

TABLE I: Performance of AF detection from Photoplethysmography data. Lowest performance for each metric is shown in gray while the highest performance is **bolded**

	Sensitivity	Specificity	Precision	F1	AUC	MCC
Shen <i>et al.</i> , 2019 [13]	0.664	0.819	0.706	0.684	0.806	0.489
Torres <i>et al.</i> , 2020 [15] (<i>Deepbeat</i>)	0.803	0.568	0.548	0.652	0.774	0.370
Torres <i>et al.</i> , 2020 [15] (<i>Deepbeat</i> , Excellent only)	0.688	0.845	0.498	0.580	0.841	0.474
BayesBeat	0.726	0.723	0.631	0.675	0.796	0.441
BayesBeat (uncertainty threshold = 0.05)	0.728	0.893	0.784	0.755	0.860	0.632
BayesBeat (uncertainty threshold = 0.01)	0.736	0.918	0.820	0.776	0.872	0.673

be separated first, and then the model performance can be measured only on the excellent signals. Therefore, we include its performance both in the “raw” form and in excellent signals only (denoted as “Excellent only”).

C. Results

Table I shows the summary results of different models, where we compare the sensitivity (recall), specificity, precision, F1-score, AUC, and MCC of our proposed method *BayesBeat* against state-of-the-art baselines. More specifically, we show three versions of *BayesBeat* by varying uncertainty thresholds (no threshold, 0.05, and 0.01). These variations essentially demonstrate how *BayesBeat* generates high uncertainty scores for noisy signals and filtering such signals by setting low uncertainty threshold substantially improves detection performance.

We observe that *BayesBeat*, with its uncertainty estimation capability, significantly outperforms all the state-of-the-art methods. Compared to [13], *BayesBeat* achieves 7.1% - 9.2% higher F1 score (depending on the selected uncertainty threshold). *BayesBeat* also outperforms *DeepBeat* (Torres *et al.* [15]) by a large margin (10-20% depending on *DeepBeat*’s excellent signal separation). It is noted that while *DeepBeat* achieves a 0.8 sensitivity score when no extra excellent signal separation stage is applied, this severely affects other metrics resulting in the lowest performance (Specificity, AUC, MCC) rendering it unsuitable for any practical application.

Furthermore, we observe that as we filter out signals beyond selected thresholds, the performance increases significantly. This phenomenon indicates that signals with high noise usually results in high uncertainty scores. In summary, *BayesBeat* consistently outperforms the state-of-the-art methods, and at the same time provides an uncertainty estimate of the results based on the signal noise, which indicates the efficacy and robustness of our proposed approach.

VI. MODEL ANALYSIS

A. Transformed feature map visualization

Figure 3 shows the t-SNE visualization [35] of the transformed features from the linear layer of our network. For this visualization, we channel the test set through our network with an uncertainty threshold of 0.05. We can see the separation between the AF and non-AF records is quite prominent in this transformed feature space generated by our model. While the non-AF and AF records form separate clusters, in the top left part we can see another small cluster of AF records which is

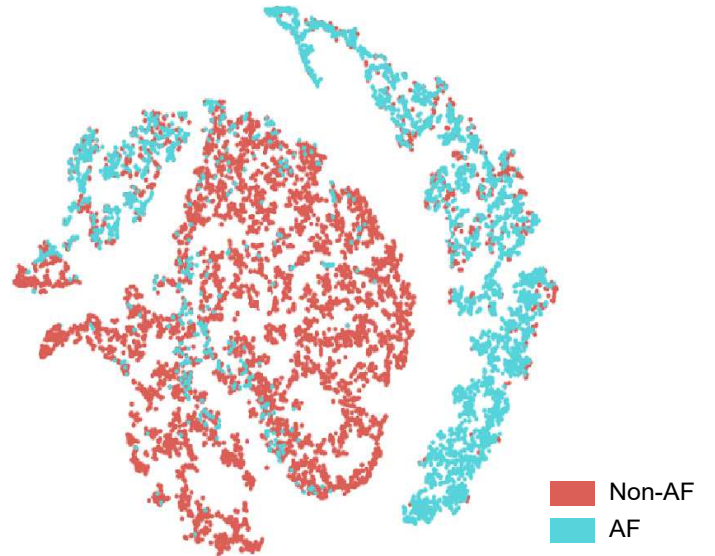


Fig. 3: t-SNE visualization of the transformed feature map from the linear layer of our network. A prominent separation between the Non-AF and AF records in this feature space demonstrates the potency of *BayesBeat*

situated relatively closer to the Non-AF cluster. These are the records for which the network is relatively less confident about whether the rhythm irregularity is due to Atrial Fibrillation or from the input noise. Thereby, our model places these data in a separate cluster. This demonstrates that *BayesBeat* effectively learns to distinguish between AF and non-AF PPG records even in challenging situations.

B. Uncertainty Estimation

As discussed, uncertainty estimation is a vital part of our model which makes it robust against PPG signal noise. In Figure 4, we present a few representative signals from the test set and the generated uncertainty scores from our model. We can see that signal (a) and signal (b) in this figure are heavily perturbed from input noise losing almost all input features that can be used for AF detection. In this case, our model generates high uncertainty scores (0.242 and 0.246) indicating that it is less certain about the decision from these inputs. On the other hand, signal (c) and signal (d) are comparably less noisy, and the beat patterns are also clearly visible, which is the key information required for AF detection. Here, our model also generates very low uncertainty scores (0.004 and

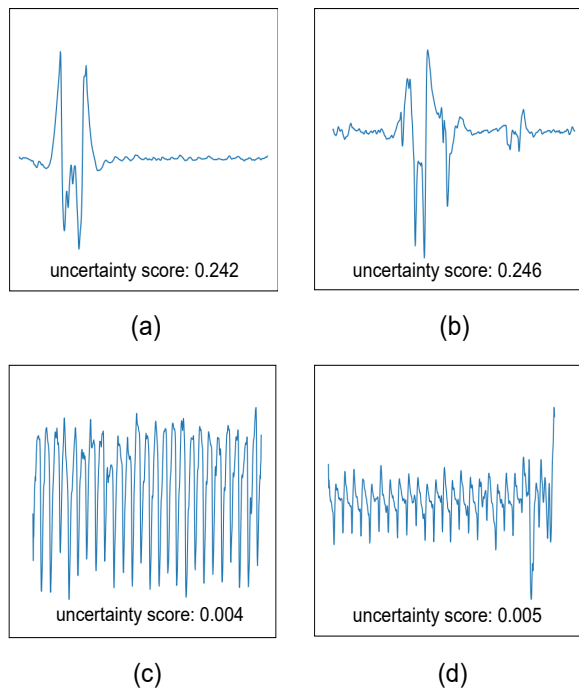


Fig. 4: Uncertainty scores of different types of signals from our test set. Signal (a) and (b) got heavily perturbed from input noise. Consequently, our model generates high uncertainty scores. Signal (c) and (d) on the other hand are less noisy, and our model thus generates very low uncertainty scores.

0.005) demonstrating that *BayesBeat* is robust against input noise.

C. Model performance in different uncertainty thresholds

In Figure 5, we present the performance of our model (F1-score and AUC) in different uncertainty thresholds. As we decrease the threshold value, the performance of the model gradually increases. Setting the uncertainty threshold to 0.01 increases the F1-score by 10% and AUC by 8% over no thresholding. Furthermore, this uncertainty scoring scheme can be very useful for commercial smartwatches, where system manufacturers can determine the best balance between performance and rate of noisy signal filtration. These uncertainty scores can also be used for weighted averaging the decisions for the signal segments collected from a specific user to provide a potential warning about possible Atrial Fibrillation.

VII. CONCLUSION

In this paper, we have proposed a novel Bayesian deep learning based approach *BayesBeat* for detection of Atrial Fibrillation from smartwatch Photoplethysmography (PPG) signals. *BayesBeat* can gracefully handle inherent input noise, which makes it suitable for deployment in consumer wearable devices that are vulnerable to motion artifacts. Our extensive experiments with the largest available dataset show that *BayesBeat* outperforms all the state-of-the-art PPG based AF detection approaches by a considerable margin. At the same time, *BayesBeat* requires only 180K parameters compared to

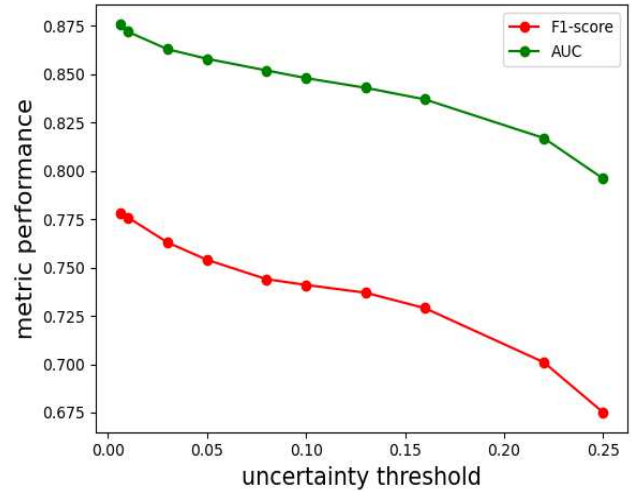


Fig. 5: F1 score and AUC of our model in different uncertainty thresholds

several million parameters in traditional deep learning models. In the future, we plan to deploy our model in commercially available smartwatches and test the real-time AF detection performance. Since the performance of Bayesian deep learning models also depend on the initially chosen prior, we also plan to experiment with different priors to attain even better performance from our model.

VIII. ACKNOWLEDGEMENT

This research has been conducted at DataLab@BUET (datalab.buet.io), and funded by ICT Division, Government of the People's Republic of Bangladesh. We'd like to thank Dr. Md. Shamimur Rahman from National Heart Foundation of Bangladesh for his valuable opinion about this work.

REFERENCES

- [1] T. Pereira, N. Tran, K. Gadhomi, M. M. Pelter, D. H. Do, R. J. Lee, R. Colorado, K. Meisel, and X. Hu, "Photoplethysmography based atrial fibrillation detection: A review," *NPJ digital medicine*, vol. 3, no. 1, pp. 1–12, 2020.
- [2] A.-M. Tăuțan, A. Young, E. Wentink, and F. Wieringa, "Characterization and reduction of motion artifacts in photoplethysmographic signals from a wrist-worn device," in *2015 37th Annual International Conference of the IEEE Engineering in Medicine and Biology Society (EMBC)*. IEEE, 2015, pp. 6146–6149.
- [3] Y. Zhang, S. Song, R. Vullings, D. Biswas, N. Simões-Capela, N. Van Helleputte, C. Van Hoof, and W. Groenendaal, "Motion artifact reduction for wrist-worn photoplethysmograph sensors based on different wavelengths," *Sensors*, vol. 19, no. 3, p. 673, 2019.
- [4] M. Nitzan, A. Romem, and R. Koppel, "Pulse oximetry: fundamentals and technology update," *Medical Devices (Auckland, NZ)*, vol. 7, p. 231, 2014.
- [5] A. L. Ries, L. M. Prewitt, and J. J. Johnson, "Skin color and ear oximetry," *Chest*, vol. 96, no. 2, pp. 287–290, 1989.
- [6] T. Shimazaki, Y. Kuwahara, M. Kimoto, S. Hara, and H. Yomo, "Effect of position and fastening belt pressure on the accuracy of ppg-based heart rate sensor," in *2018 40th Annual International Conference of the IEEE Engineering in Medicine and Biology Society (EMBC)*. IEEE, 2018, pp. 4323–4326.

- [7] S.-M. Shan, S.-C. Tang, P.-W. Huang, Y.-M. Lin, W.-H. Huang, D.-M. Lai, and A.-Y. A. Wu, "Reliable ppg-based algorithm in atrial fibrillation detection," in *2016 IEEE Biomedical Circuits and Systems Conference (BioCAS)*. IEEE, 2016, pp. 340–343.
- [8] M. Lemay, S. Fallet, P. Renevey, J. Solà, C. Leupi, E. Pruvot, and J.-M. Vesin, "Wrist-located optical device for atrial fibrillation screening: A clinical study on twenty patients," in *2016 Computing in Cardiology Conference (CinC)*. IEEE, 2016, pp. 681–684.
- [9] V. D. Corino, R. Laureanti, L. Ferranti, G. Scarpini, F. Lombardi, and L. T. Mainardi, "Detection of atrial fibrillation episodes using a wristband device," *Physiological measurement*, vol. 38, no. 5, p. 787, 2017.
- [10] S. Fallet, M. Lemay, P. Renevey, C. Leupi, E. Pruvot, and J.-M. Vesin, "Can one detect atrial fibrillation using a wrist-type photoplethysmographic device?" *Medical & Biological Engineering & Computing*, vol. 57, no. 2, pp. 477–487, 2019.
- [11] G. H. Tison, J. M. Sanchez, B. Ballinger, A. Singh, J. E. Olgin, M. J. Pletcher, E. Vittinghoff, E. S. Lee, S. M. Fan, R. A. Gladstone *et al.*, "Passive detection of atrial fibrillation using a commercially available smartwatch," *JAMA cardiology*, vol. 3, no. 5, pp. 409–416, 2018.
- [12] A. Aliamiri and Y. Shen, "Deep learning based atrial fibrillation detection using wearable photoplethysmography sensor," in *2018 IEEE EMBS International Conference on Biomedical & Health Informatics (BHI)*. IEEE, 2018, pp. 442–445.
- [13] Y. Shen, M. Voisin, A. Aliamiri, A. Avati, A. Hannun, and A. Ng, "Ambulatory atrial fibrillation monitoring using wearable photoplethysmography with deep learning," in *Proceedings of the 25th ACM SIGKDD International Conference on Knowledge Discovery & Data Mining*, 2019, pp. 1909–1916.
- [14] S. Xie, R. Girshick, P. Dollár, Z. Tu, and K. He, "Aggregated residual transformations for deep neural networks," in *Proceedings of the IEEE conference on computer vision and pattern recognition*, 2017, pp. 1492–1500.
- [15] J. Torres-Soto and E. A. Ashley, "Multi-task deep learning for cardiac rhythm detection in wearable devices," *npj Digital Medicine*, vol. 3, no. 1, pp. 1–8, 2020.
- [16] M. Elgendi, "Optimal signal quality index for photoplethysmogram signals," *Bioengineering*, vol. 3, no. 4, p. 21, 2016.
- [17] J. Lee, Y. Nam, D. D. McManus, and K. H. Chon, "Time-varying coherence function for atrial fibrillation detection," *IEEE Transactions on Biomedical Engineering*, vol. 60, no. 10, pp. 2783–2793, 2013.
- [18] L. Krivoshei, S. Weber, T. Burkard, A. Maseli, N. Brasier, M. Kühne, D. Conen, T. Huebner, A. Seeck, and J. Eckstein, "Smart detection of atrial fibrillation," *Europace*, vol. 19, no. 5, pp. 753–757, 2017.
- [19] S. K. Bashar, D. Han, A. Soni, D. D. McManus, and K. H. Chon, "Developing a novel noise artifact detection algorithm for smartphone ppg signals: Preliminary results," in *2018 IEEE EMBS International Conference on Biomedical & Health Informatics (BHI)*. IEEE, 2018, pp. 79–82.
- [20] J. W. Chong, C. H. Cho, N. Esa, D. D. McManus, and K. H. Chon, "Motion and noise artifact-resilient atrial fibrillation detection algorithm for a smartphone," in *2016 IEEE-EMBS International Conference on Biomedical and Health Informatics (BHI)*. IEEE, 2016, pp. 591–594.
- [21] S.-C. Tang, P.-W. Huang, C.-S. Hung, S.-M. Shan, Y.-H. Lin, J.-S. Shieh, D.-M. Lai, A.-Y. Wu, and J.-S. Jeng, "Identification of atrial fibrillation by quantitative analyses of fingertip photoplethysmogram," *Scientific reports*, vol. 7, p. 45644, 2017.
- [22] S. Nemat, M. M. Ghassemi, V. Ambai, N. Isakadze, O. Levantsevych, A. Shah, and G. D. Clifford, "Monitoring and detecting atrial fibrillation using wearable technology," in *2016 38th Annual International Conference of the IEEE Engineering in Medicine and Biology Society (EMBC)*. IEEE, 2016, pp. 3394–3397.
- [23] T. Schäck, Y. S. Harb, M. Muma, and A. M. Zoubir, "Computationally efficient algorithm for photoplethysmography-based atrial fibrillation detection using smartphones," in *2017 39th Annual International Conference of the IEEE Engineering in Medicine and Biology Society (EMBC)*. IEEE, 2017, pp. 104–108.
- [24] M.-Z. Poh, Y. C. Poh, P.-H. Chan, C.-K. Wong, L. Pun, W. W.-C. Leung, Y.-F. Wong, M. M.-Y. Wong, D. W.-S. Chu, and C.-W. Siu, "Diagnostic assessment of a deep learning system for detecting atrial fibrillation in pulse waveforms," *Heart*, vol. 104, no. 23, pp. 1921–1928, 2018.
- [25] C. Blundell, J. Cornebise, K. Kavukcuoglu, and D. Wierstra, "Weight uncertainty in neural networks," *arXiv preprint arXiv:1505.05424*, 2015.
- [26] D. P. Kingma, T. Salimans, and M. Welling, "Variational dropout and the local reparameterization trick," in *Advances in neural information processing systems*, 2015, pp. 2575–2583.
- [27] Y. Gal and Z. Ghahramani, "Dropout as a bayesian approximation: Representing model uncertainty in deep learning," in *international conference on machine learning*, 2016, pp. 1050–1059.
- [28] L. V. Jospin, W. Buntine, F. Boussaid, H. Laga, and M. Bennamoun, "Hands-on bayesian neural networks-a tutorial for deep learning users," *ACM Comput. Surv.*, vol. 1, no. 1, 2020.
- [29] Y. Kwon, J.-H. Won, B. J. Kim, and M. C. Paik, "Uncertainty quantification using bayesian neural networks in classification: Application to ischemic stroke lesion segmentation," 2018.
- [30] F. Wenzel, K. Roth, B. S. Veeling, J. Świątkowski, L. Tran, S. Mandt, J. Snoek, T. Salimans, R. Jenatton, and S. Nowozin, "How good is the bayes posterior in deep neural networks really?" *arXiv preprint arXiv:2002.02405*, 2020.
- [31] C. K. Sønderby, T. Raiko, L. Maaløe, S. K. Sønderby, and O. Winther, "Ladder variational autoencoders," in *Advances in neural information processing systems*, 2016, pp. 3738–3746.
- [32] K. Shridhar, F. Laumann, and M. Liwicki, "Uncertainty estimations by softplus normalization in bayesian convolutional neural networks with variational inference," *arXiv preprint arXiv:1806.05978*, 2018.
- [33] D. P. Kingma and J. Ba, "Adam: A method for stochastic optimization," *arXiv preprint arXiv:1412.6980*, 2014.
- [34] S. Boughorbel, F. Jarray, and M. El-Anbari, "Optimal classifier for imbalanced data using matthews correlation coefficient metric," *PLoS one*, vol. 12, no. 6, p. e0177678, 2017.
- [35] L. v. d. Maaten and G. Hinton, "Visualizing data using t-sne," *Journal of machine learning research*, vol. 9, no. Nov, pp. 2579–2605, 2008.